High sensitive and selective C-reactive protein detection by means of lossy mode resonance based optical fiber devices

P. Zubiate[a, *]

pablo.zubiate@unavarra.es

C.R. Zamarreño[a, b]

P. Sánchez[a]

I.R. Matias[a, b]

F.J. Arregui[a, b]

[a]UPNA Sensors Group, Electrical and Electronic Engineering Department, Public University of Navarra, Edificio de Los Tejos, Campus Arrosadia, 31006 Pamplona, Spain

[b]Institute of Smart Cities, Jeronimo de Ayanz Center, Campus Arrosadia, 31006 Pamplona, Spain

*Corresponding author.

Abstract

This work presents the development of high sensitive, selective, fast and reusable C-reactive protein (CRP) aptasensors. This novel approach takes advantage of the utilization of high sensitive refractometers based on Lossy Mode Resonances generated by thin indium tin oxide (ITO) films fabricated onto the planar region of D-shaped optical fibers. CRP selectivity is obtained by means of the adhesion of a CRP specific aptamer chain onto the ITO film using the Layer-by-Layer (LbL) nano-assembly fabrication process. The sensing mechanism relies on resonance wavelength shifts originated by refractive index variations of the aptamer chain in presence of the target molecule. Fabricated devices show high selectivity to CRP when compared with other target molecules, such as urea or creatinine, while maintaining a low detection limit (0.0625 mg/L) and fast response time (61 s). Additionally, these sensors show a repetitive response for several days and are reusable after a cleaning process in ultrapure water.

Keywords: Biosensors; C-reactive protein; Optical fiber; Lossy mode resonance; D-shaped

1 Introduction

C-reactive protein (CRP) is an acute-phase protein of hepatic origin found in blood plasma. CRP concentration level rise up to three orders in response to inflammation (Cem and Irving, 1999; Thompson et al., 1999). CRP measuring is not specific for any condition but it is a fairly sensitive biomarker of inflammation and has been proven very useful in determining disease progress as well as the effectiveness of treatments in inflammations, infections, tissue necrosis, surgery, burns, cancer, cardiovascular diseases or coronary heart disease risk (Danesh et al., 2004; Lau et al., 2005; Llombart et al., 2013; Pepys and Hirschfield, 2003). Thus, CRP has emerged as an effective disease biomarker in human body with an even more sensitive and accurate reflection of the acute phase response than the ESR (Erythrocyte Sedimentation Rate) in some cases (Liu et al., 2013).

The median concentration of CRP is 0.8 mg/L and always less than 12 mg/L in apparently healthy individuals with higher values in elder people. In particular, the risk of developing cardiovascular disease has been quantified as low below 1.0 mg/L, as average between 1.0 and 3.0 mg/L and high above 3.0 mg/L. Common techniques used for CRP measurement comprise ELISA, immunoturbidimetry, nephelometry, rapid immunodiffusion, and visual agglutination with detection ranges between 0.1 and 0.2 mg/L (Centi et al., 2009). Other techniques, such as surface plasmon resonance (SPR) (Meyer et al., 2006), quartz crystal microbalance (QCM) (Kim et al., 2009), piezoelectric micro-cantilever (Wee et al., 2005), electrochemistry (Centi et al., 2009), electrochemical impedance spectroscopy (Bryan et al., 2013), micro particle-tracking velocimetry (MPTV) (Fan et al., 2010) and fiber bragg gratings (FBGs) have been also described in literature (S. Sridevi et al., 2015a, 2015b).

Previous techniques have been proven to successfully detect CRP but present different drawbacks. For example, antibody-based techniques are sensitive to circumstance and its activity can be unstable.

Furthermore, the preparation of monoclonal and polyclonal antibodies varies depending on the immune response in different animals and causes the variable specificity and sensitivity of CRP between different methods. ELISA and other photometric methods can be distorted by the color and composition of the medium used in assays. CRP concentration begins to rise in the body usually 6–12 h after an inflammatory stimulus and peak around 48–96 h after the event while some techniques require several hours or even a day and are not recommended for early stage CRP identification or to perform a continuous tracking of patient evolution.

In this work we present the utilization of lossy mode resonance (LMR) based optical fiber devices combined with a highly selective sensing layer for fast CRP detection at low concentrations. Fiber optic biosensors have been widely described in literature as an alternative cost-effective, compact, real time and rapid detection solution (Ecke et al., 2011; Sridevi et al., 2015a, 2015b; Wolfbeis, 2008; Zamarreño et al., 2013). Among them, LMR-based optical fiber devices have been presented as a high sensitive and versatile label-free refractometers (Arregui et al., 2016; Del Villar et al., 2010; Zubiate et al., 2015). The biosensor consist of the combination of LMR-based devices with the adequate sensing coating, the refractive index of which varies with the selected target. In this case, the sensing layer comprises a CRP-selective aptamer. Aptamers have become increasingly important because they possess unprecedented advantages compared to biosensors using antibodies or enzymes, such as the in vitro selection and synthesis process, stability, long lifetime or regeneration among others (Feng et al., 2014). The high affinity of aptamers to their target molecules can be associated to their capability of folding upon their target molecule, which is known as conformational change, and derives in refractive index measurable changes (Ellington and Szostak, 1990).

The first part of the manuscript describes the device fabrication process followed by the characterization of the response of the device for different CRP concentrations, repeatability and reusability test, response time measurement and concluding with the selectivity experiments.

2 Materials and methods

2.1 Materials and sample preparation

Poly (allylamine) hydrochloride (PAH) (Mw~65.000) and Poly (sodium 4-styrenesulfonate)(PSS) (Mw~70.000) were purchased from Sigma-Aldrich Inc. PAH aqueous solution was used as the polycationic solution and PSS aqueous solution was used as the polyanionic solution. Ultrapure water (18.1 MΩ/cm) was obtained from a Barnstead Inc. water purification system. Both, PAH and PSS solution were fabricated at 2 mg/ml and adjusted at pH 6.0 (Crinson Inc. pH-meter) (Crison Inc.) by adding hydrochloric acid or sodium hydroxide drops as necessary.

The reagents Tris (hydroxymethyl)aminomethane, NaCl and $CaCL_2$ for Tris Buffer Saline (TBS) preparation were obtained from Sigma-Aldrich Inc. TBS solution contains a concentration of 50 mM TRIS, 150 mM NaCl and 5 mM $CaCl_2$.

DNA-aptamer sequence specific for C-Reactive protein (CRP) (5′-GGCAGGAAGACAAACATATAATTGAGATCGTTTGATGACTTTGTAAGAGTGTGGAATGGTCTGTGGTGCTGT-3′) (Huang et al., 2010) is HPLC purified and was purchased from Thermo Scientific. The DNA was dissolved in Tris Buffer Solution pH 7.6.

C-reactive was acquired from Cell-Biolabs. Urea and Creatinine, which are used as interfering factors, were purchased from Sigma Aldrich. CRP in TBS solution at concentrations ranging from 0.0625 mg/L to 2 mg/L are used for sensitivity measurements. Similarly, urea and creatinine in TBS solution at concentrations ranging from 0.0625 mg/L to 20 mg/L have been prepared for selectivity measurements.

2.2 LMR sensor fabrication

The fabricated optical sensor platform has been described in previous works of our group (Arregui et al., 2016; ~~P.~~ Zubiate et al., 2015). The LMR-based device consists of a thin ITO film fabricated onto the planar region of a side polished optical fiber. D-shaped fibers were obtained from Phoenix Photonics LTD. These fibers consisted of standard single mode fibers (Corning®SMF-28) with a cladding/core diameter of 125/8.2 μm, a polished length of 17 mm and an attenuation peak of 5 dB at 1550 nm in high refractive index oil (1.5). D-shape optical fibers were firstly cleaned using a plasma treatment (Plasma ACE 1 from Gala Instrumente) for approximately 10 min before the ITO coating deposition process. 100 nm thick ITO coatings were fabricated using a DC sputtering machine (K675XD from Quorum Technologies) with a partial pressure of argon of 9×10^{-2} mbar and intensity of 150 mA. The obtained structure was used as substrate for the fabrication of the receptor layer.

2.3 Experimental setup

The experimental setup consisted of a broadband light source (HP_83437A - SLED), with an emission range from 1150 to 1680 nm, connected to a depolarizer (from Phoenix Photonics) in order to scramble the polarization of the light source. The depolarizer output is connected to a polarization controller (Agilent 9169A) used to adjust the polarization of the light that goes through the sensitive region. Finally, the output of the sensor is attached to an OSA (HP- 86142A) in order to monitor the response of the device (see Fig. 1a).

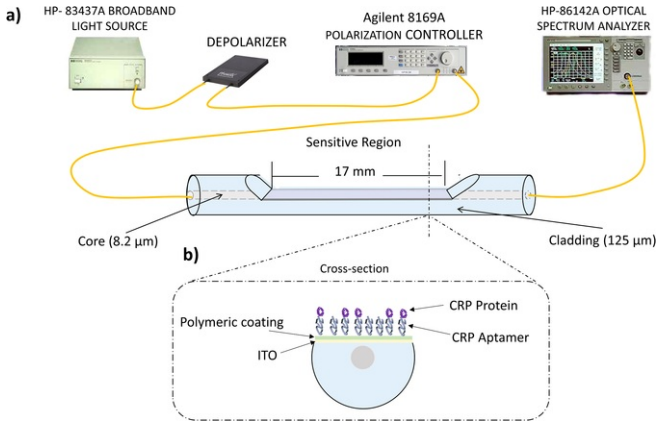

Fig. 1 a) Experimental setup and detail of the sensitive region b) a schematic representation of the aptamer immobilization on the D-shaped optical fiber.

alt-text: Fig. 1.

All experiments were performed at room temperature. The climatic conditions were stabilized at 23 °C of temperature and relative humidity of 35% during the fabrication and measuring processes.

3 Results

LMRs have been obtained with different optical fiber configurations, such as cladding removed multimode fibers (Zamarreño et al., 2011) or tapered fibers (Socorro et al., 2012) but D-shaped optical fibers have proven to obtain the highest sensitivity and narrower LMRs up to now (Arregui et al., 2016). In particular, the narrow spectral widths of LMRs are directly associated to singlemode structures and can be explained by considering the condition for maximum coupling from a core mode to a lossy mode in a thin-film (Grzegorzewski and Szustakowski, 1993; Socorro et al., 2014). Furthermore, the characteristic asymmetry of the planar region of D-shaped fibers enables to differentiate between TM and TE polarizations and permits to obtain separately the LMRs associated with both polarizations LMR_{TM} and LMR_{TE}. Since LMR_{TM} and LMR_{TE} are positioned at different wavelengths it is required the utilization of polarized light to obtain a single resonance. On the other hand, the utilization of non-polarized light could mask the spectral response because the detector (OSA in this case) does not distinguish between both polarizations. In this case, we use TE polarization. More specifically, we use TE polarization of the first LMR (LMR_{TE}). LMRs are highly sensitive to surrounding medium refractive (SMRI) index variations. Therefore, it can be obtained an accurate determination of the SMRI by means of the determination of LMR wavelength shift. Intensity modulation could be used to measure the SMRI, but this technique presents several drawbacks associated to optical power fluctuations such as the ageing of light source and movements or bending of the fiber, which require a more elaborated setup. In contrast, LMR wavelength shift monitoring used in this work overrides all this problems. In summary, we have employed wavelength shift detection on LMR-based devices fabricated onto D-shaped optical fibers because of their high sensitivity to SMRI variations, narrow width, the possibility to differentiate between TE and TM polarizations and the simplicity of wavelength detection, which does not require a complex setup or optical power source reference.

3.1 Fabrication of the sensing layer

ITO coated D-shaped optical fibers have been proven as highly sensitive refractometers (Arregui et al., 2016; ~~P~~ Zubiate et al., 2015). Thus, the fabrication of a selective sensing layer, the refractive index of which varies with the target, onto the ITO coating could be used to measure specific interactions as for example between CRP-aptamer and CRP.

The receptor layer, fabricated using the LbL technique (Cooper et al., 2011; Wang et al., 2007), consisted of a structure formed by four PAH and PSS bilayers followed by the CRP-aptamer layer as it is schematically represented in Fig. 1b. In order to maximize the surface concentration of the aptamer immobilized onto the fiber and the detection of CRP-aptamer, optimal parameters of the structure polymeric need to be studied. Several experiments were performed for different bilayers number and it was decided that four bilayers was the best choice for several reasons as follow. Increasing the number of bilayers increases the polymer thickness and the ability to detect the aptamer-CRP binding (reduces the sensitivity). On the other hand, reducing the number of bilayers does not permit to obtain a homogeneous surface coverage for an adequate polymer-DNA binding. In addition, studies reported in (Wang et al., 2007) confirm that polymeric structure and aptamer layer was successfully immobilized onto the fiber as well as the results obtained during our experiment. These studies are based on measurements of film thickness with the FESEM (Wang et al., 2007). The fabrication process comprises a first immersion step of the ITO coated D-shaped optical fiber in 1 M KOH during 10 min followed by a washing in ultrapure water in order to acquire a prior negative charge.

Afterwards, the fiber is immersed into the positively charged polymer (PAH) and then into the negatively charged polymer (PSS) for 3 min each immersion. The substrates are rinsed in ultrapure water for 1 min after each layer. The structure obtained after this process is known as a bilayer. CRP-aptamer is immobilized after the fabrication of 4 bilayers. Due to the negative charge of single DNA chain the sensor is first immersed in the PAH solution for 3 min and then into the CRP-aptamer solution (1 μM) for 10 min. After this process, the fabrication of the sensor is completed.

The immobilization of the receptor structure onto ITO coated D-shape optical fiber and the detection of CRP are monitored using the setup shown in Fig. 1a. Firstly, the LbL fabrication process is monitored in order to successfully guarantee the aptamer immobilization onto the sensitive region. Fig. 2 shows the transmittance response of the device as a function of the number of bilayers added onto the ITO D-shape fiber. Here, the LMR shows a redshift as a function of the number of bilayers added onto the ITO coating, which assures a correct immobilization of the aptamer onto the sensor. In particular, the resonance wavelength shifts a total of 34 nm (from 1387 nm to 1421 nm) during the polymeric structure fabrication process and 24 nm (from 1421 nm to 1445 nm) after the aptamer layer fabrication. In Fig. 2b it can be observed a linear response of the resonance wavelength shift for the fabrication of the polymeric structure. This indicates that the polymer thickness growth is constant and equal for each bilayer (34 nm). However, the response after the aptamer immobilization is not linear (24 nm). This corroborates that the aptamer has been successfully immobilized onto the sensor but the contribution of the aptamer to the coating is higher than that of the polymer in terms of optical thickness. Since resonance shifts are associated to refractive variations in the surrounding medium it can be concluded that either the refractive index or the thickness of the aptamer layer is larger than a single polymeric layer. In the same manner, the overall contribution of the polymeric structure is larger than the single aptamer layer.

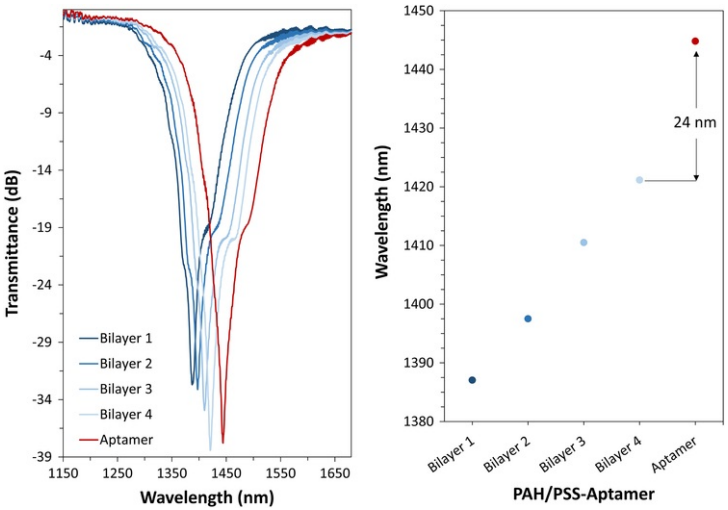

Fig. 2 Transmission spectrum of the LMR at each stage of immobilization of aptamer on the sensing region.

alt-text: Fig. 2.

3.2 Detection of CRP

Different types of experiments are performed in order to successfully corroborate the detection of CRP protein. Initially, the sensitive region of the device is dipped in CRP solutions with concentrations between 0.0625 mg/L and 1 mg/L. Fig. 3 represents the transmittance response of the sensor when it is subjected to different CRP concentrations. Here, it can be seen that the spectral response of the sensor and the resonance wavelength changes with the concentration of CRP or, in other words, the resonance wavelength shifts towards higher wavelengths as the concentration of CRP increases. In particular, it can be seen a total wavelength shift of 35 nm for CRP concentrations varying from buffer to 1 mg/L, which reveals that the sensor can successfully detect CRP at very low concentrations. The response of the device can be fitted well to the exponential logarithmic equation in Fig. 3 with R^2 value of 0.9968. From the response approximation equation obtained in Fig. 3 it can be calculated the sensitivity of the device in the vicinity of the studied concentrations. The sensitivities have been calculated from the slope of the tangent at the different concentrations using the first derivative of the logarithmic approximation. The sensitivities are 169.93, 84.968, 42.484, 21.242 and 10.621 nm/(mg/L) for 0.0625, 0.125, 0.25, 0.5 and 1 mg/L respectively. This means that in the best case (concentration of 0.0625 mg/L), the OSA used in this work with a 2.0 nm resolution can distinguish concentrations with a difference of ±0.006 mg/L of C reactive protein. The utilization of a better resolution equipment and calibrated solutions at lower concentrations would allow us to improve this value as well as the level of detection (LOD).

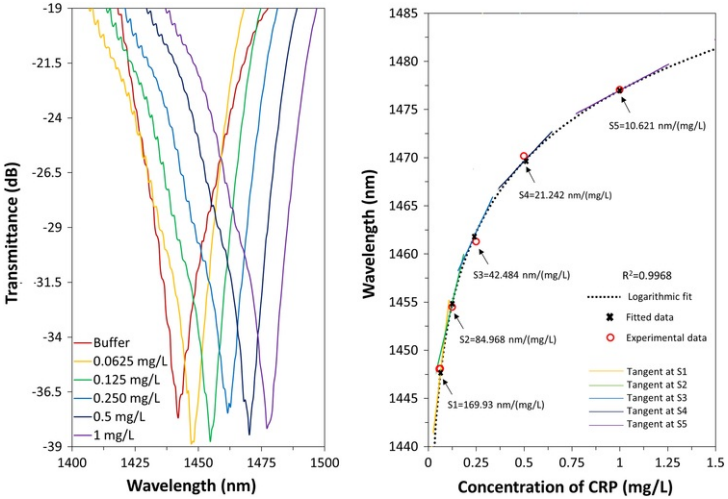

Fig. 3 Spectral response of the sensor when the sensitive region is exposed to different concentration of CRP.

alt-text: Fig. 3.

The dynamical response and reusability of the device is also tested. Here, it is recorded the spectral response of the devices in order to obtain the resonance wavelength while the devices are subjected to different concentrations of CRP for different periods of time. Each step of the interactions between the aptamer and the specific protein is monitored in real-time using the experimental setup in Fig. 1. The spectral response is taken every minute as it is shown in Fig. 4. It can be seen that the resonance wavelength shifts at each CRP concentration showing good stability and a repetitive response. Here, it is also important to observe that the response of the device is stable between the immersion in the CRP solution and the immersion in buffer. This means that CRP is tightly linked to its complementary CRP-aptamer showing a negligible change in the resonance wavelength when the device is immersed in the buffer control solutions. This confirms that the resonance wavelength shift is directly related to the refractive index variation of the sensitive layer due to the interaction between the aptamer chain and the protein and not to small variations in the RI of the solutions. It is important to remark that Fig. 4 shows the response of the same device for different days after a recovery process in ultrapure water overnight and it retains the same sensitivity. In order to corroborate that the displacement of the resonance is due to the interaction between CRP and aptamer, the refractive index of the CRP solutions was measured with the refractometer 30GS from METTLER TOLEDO Inc. The refractive index is 1.3350 for all solutions. This indicates that the displacement is not produced by the change of the refractive index of the solution.

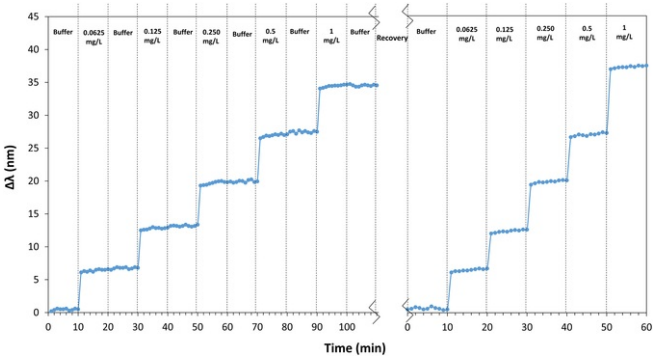

Fig. 4 Dynamical response of the device.

alt-text: Fig. 4.

The response time of the device is obtained by monitoring the output power at 1442 nm every 500 ms while it is immersed in buffer and CRP at 0.125 mg/L. From Fig. 5 it can be observed a response time of 61 s. Although the wavelength detection is a more robust and immune to power optical power fluctuations, the experimental measuring setup that is used (see Fig. 1) has its response time conditioned by the acquisition time of the OSA. In particular, the

OSA requires around 60 s to obtain a single measurement of the studied spectral range (1400–1500 nm), which is not too high but does not enable to perform precise response time measurements. For this reason the OSA has been configured to acquire the optical power at a single wavelength (wavelength near the resonance wavelength in this case). In this case it is required the utilization of a very stable setup, avoiding vibrations or temperature fluctuations, which could alter the measurement. In this way it is possible to obtain the response time of the device.

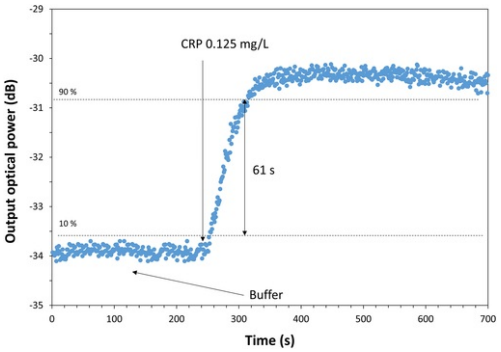

Fig. 5 Response time of the sensor.

alt-text: Fig. 5.

In order to study the selectivity of the biosensors, they are subjected to different solutions in presence of other molecules, such as urea and creatinine at the same concentrations used with CRP. Fig. 6 shows the LMR wavelength shift values for different concentrations of CRP, urea and creatinine. The shift in resonance wavelength as a function of urea and creatinine solutions in each case are shown in the inset of Fig. 6 along with corresponding error bar at each point. The values of LMR shifts for urea and creatinine is less than 1 nm. A negligible change in the resonance wavelength can be observed when the device is immersed in urea and creatinine solutions, which confirms that the sensitive layer (CRP-aptamer) is highly selective to CRP. The presence of other substances, such as urea and creatinine does not modify the response of the device particularly. These results indicate that the non-specific proteins tested do not attach correctly to the CRP-aptamer and corroborate again that the resonance wavelength shift is directly associated to the interaction of the C-reactive protein with aptamer.

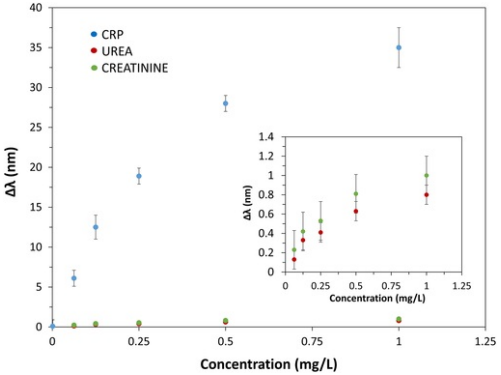

Fig. 6 The shift in wavelength when the sensitive region is exposed of different concentration of CRP, Urea and Creatinine.

alt-text: Fig. 6.

Four identical sensors were fabricated in order to observe the repeatability and reproducibility of these experiments. So, the experiment was replicated four times for the same concentration of CRP, urea and creatinine, and averaged, being obtained a maximum error bar for the measured wavelength shifts of ±3 nm. These results indicate that the sensor is highly reproducible.

The limit of detection are compared with other methods reported in the literature. A limit of detection of 0.01 mg/L, 1 mg/L, 0.00013 mg/L, 0.01 mg/L, 0.054 mg/L, 0.018 mg/L, 1 mg/L has been achieved in fiber Bragg gratings (S. Sridevi et al., 2015a, 2015b), surface plasmon resonance (SPR) (Meyer et al., 2006), quartz crystal microbalance (QCM) (Kim et al., 2009), piezoelectric micro-cantilever (Wee et al., 2005), electrochemistry (Centi et al., 2009), electrochemical impedance spectroscopy (Bryan et al., 2013) and micro particle-tracking velocimetry (MPTV) (Fan et al., 2010) respectively. From the results below, fabricated LMR-based optical fiber devices are a good and

competitive when compared with previous works in the field of optical fiber biosensors and present a good opportunity of improvement for future works.

4 Conclusions

An optical fiber CRP biosensor based on Lossy Mode Resonances (LMR) has been fabricated and characterized. LMRs devices based on thin ITO films fabricated onto D-shaped optical fibers have been used as a versatile sensing platform for the biosensor fabrication. In particular, fabricated devices can detect concentrations of CRP of 0.0625 mg/L or even lower, which is within the same order of magnitude of that from other works that employ complex techniques. The experimental results presented in this work show that the biosensor has good sensitivity to low CRP concentrations. In addition, the biosensor shows high specificity to CRP and negligible interactions with other molecules showing fast response time (61 sonds) good repeatability and reusability between different days. Moreover, selectivity and response time results provided demonstrate the feasibility of the proposed optical biosensor to be easily used in real conditions where the detection of low CRP concentrations is a general practice.

In conclusion, the results presented here demonstrate that the described optical sensing configuration combined with the adequate sensitive layer can be used as an alternative sensing platform for high sensitive and highly selective applications in biosensors.

Acknowledgements

This work was supported by a Pre-Doctoral Research Grant of the Public University of Navarra, Spanish Economy and Competitiveness Ministry-Feder TEC2013-43679-R and Fundación CAN2015-70221 Research Grants.

References

Arregui F.J., Del Villar I., Zamarreño C.R., Zubiate P. and Matias I.R., *Sens. Actuators B Chem.* **232**, 2016, 660–665.

Bryan T., Luo X., Bueno P.R. and Davis J.J., *Biosens. Bioelectron.* **39**, 2013, 94–98.

Cem G. and Irving K., *N. Engl. J. Med.* **340**, 1999, 448–454.

Centi S., Bonel Sanmartin L., Tombelli S., Palchetti I. and Mascini M., *Electroanalysis* **21**, 2009, 1309–1315.

Cooper K.L., Bandara A.B., Wang Y., Wang A. and Inzana T.J., *Sensors* **11**, 2011, 3004–3019.

Danesh J., Wheeler J.G., Hirschfield G.M., Eda S., Eiriksdottir G., Rumley A., Lowe G.D.O., Pepys M.B. and Gudnason V., *N. Engl. J. Med.* **350**, 2004, 1387–1397.

Del Villar I., Zamarreno C.R., Hernaez M., Arregui F.J. and Matias I.R., *J. Lightw. Technol.* **28**, 2010, 111–117.

Ecke W., Andreev A., Csaki A., Kirsch K., Schroeder K., Wieduwilt T. and Willsch R., *Proc. SPIE* 2011.

Ellington A.D. and Szostak J.W., *Nature* **346**, 1990, 818–822.

Fan Y.-J., Sheen H.-J., Liu Y.-H., Tsai J.-F., Wu T.-H., Wu K.-C. and Lin S., *Langmuir* **26**, 2010, 13751–13754.

Feng C., Dai S. and Wang L., *Biosens. Bioelectron.* **59**, 2014, 64–74.

Grzegorzewski J. and Szustakowski M., *IEE Proc. J. Optoelectron.* **140**, 1993, 247–252.

Huang C.-J., Lin H.-I., Shiesh S.-C. and Lee G.-B., *Biosens. Bioelectron.* **25**, 2010, 1761–1766.

Kim N., Kim D.-K. and Cho Y.-J., *Sens. Actuators B: Chem.* **143**, 2009, 444–448.

Lau D.C.W., Dhillon B., Yan H., Szmitko P.E. and Verma S., *Am. J. Physiol. Heart Circ. Physiol.* **288**, 2005, H2031–H2041.

Liu S., Ren J., Xia Q., Wu X., Han G., Ren H., Yan D., Wang G., Gu G. and Li J., *Am. J. Med. Sci.* **346**, 2013, 467–472.

Llombart V., García-Berrocoso T., Bustamante A., Fernández-Cadenas I. and Montaner J., *Curr. Cardiol. Rev.* **9**, 2013, 340–352.

Meyer M.H.F., Hartmann M. and Keusgen M., *Biosens. Bioelectron.* **21**, 2006, 1987–1990.

Pepys M.B. and Hirschfield G.M., *J. Clin. Investig.* **111**, 2003, 1805–1812.

Socorro A.B., Del Villar I., Corres J.M., Arregui F.J. and Matias I.R., *Sens. Actuators B Chem.* **200**, 2014, 53–60.

Socorro A.B., Villar I., Del, Corres J.M., Arregui F.J. and Matias I.R., *IEEE Sens. J.* **12**, 2012, 2598–2603.

Sridevi S., Vasu K.S., Asokan S. and Sood A.K., *Biosens. Bioelectron.* **65**, 2015a, 251–256.

Sridevi S., Vasu K.S., Asokan S. and Sood A.K., *Biosens. Bioelectron.* **65**, 2015b, 251–256.

Thompson D., Pepys M.B. and Wood S.P., *Structure* **7**, 1999, 169–177.

Wang Q., Yang X. and Wang K., *Sens. Actuators B Chem.* **123**, 2007, 227–232.

Wee K.W., Kang G.Y., Park J., Kang J.Y., Yoon D.S., Park J.H. and Kim T.S., *Biosens. Bioelectron.* **20**, 2005, 1932–1938.

Wolfbeis O.S., *Anal. Chem.* **80**, 2008, 4269–4283.

Zamarreño C.R., Hernáez M., Del Villar I., Matías I.R. and Arregui F.J., *Sens. Actuators B Chem.* **155**, 2011, 290–297.

Zamarreño C.R., Ardaiz I., Ruete L., Matias I.R. and Arregui F.J., *IEEE Sens.* **2013**, 2013, 1–4.

Zubiate P., Zamarreño C.R., Del Villar I., Matias I.R. and Arregui F.J., *Opt. Express* **23**, 2015, 8045–8050.

Highlights

- Fiber optic biosensor based on Lossy Mode Resonance (LMR) is developed for detection of C-reactive protein.
- Lossy Mode Resonances (LMRs) sensors for C-reactive protein detection.
- The sensor is based on the shift in resonance wavelength of the LMR due to the interaction of ~~C-reactive~~ protein with the aptamer.
- Fabricated devices show high selectivity to CRP, a low detection limit (0.0625 mg/L) and fast response time (61 s).

Queries and Answers

Query:

Highlights should only consist of 125 characters per bullet point, including spaces. The highlights provided are too long; please edit them to meet the requirement.

Answer: All changes have been performed accordingly.